UiT

NORGES ARKTISKE UNIVERSITET

Faculty of Science and Technology

Methane bubbles in the Arctic Ocean

Quantification, variability analysis and modelling of free and dissolved methane from the seafloor to the atmosphere

—

Pär Jansson

A dissertation for the degree of Philosophiae Doctor – May 2018

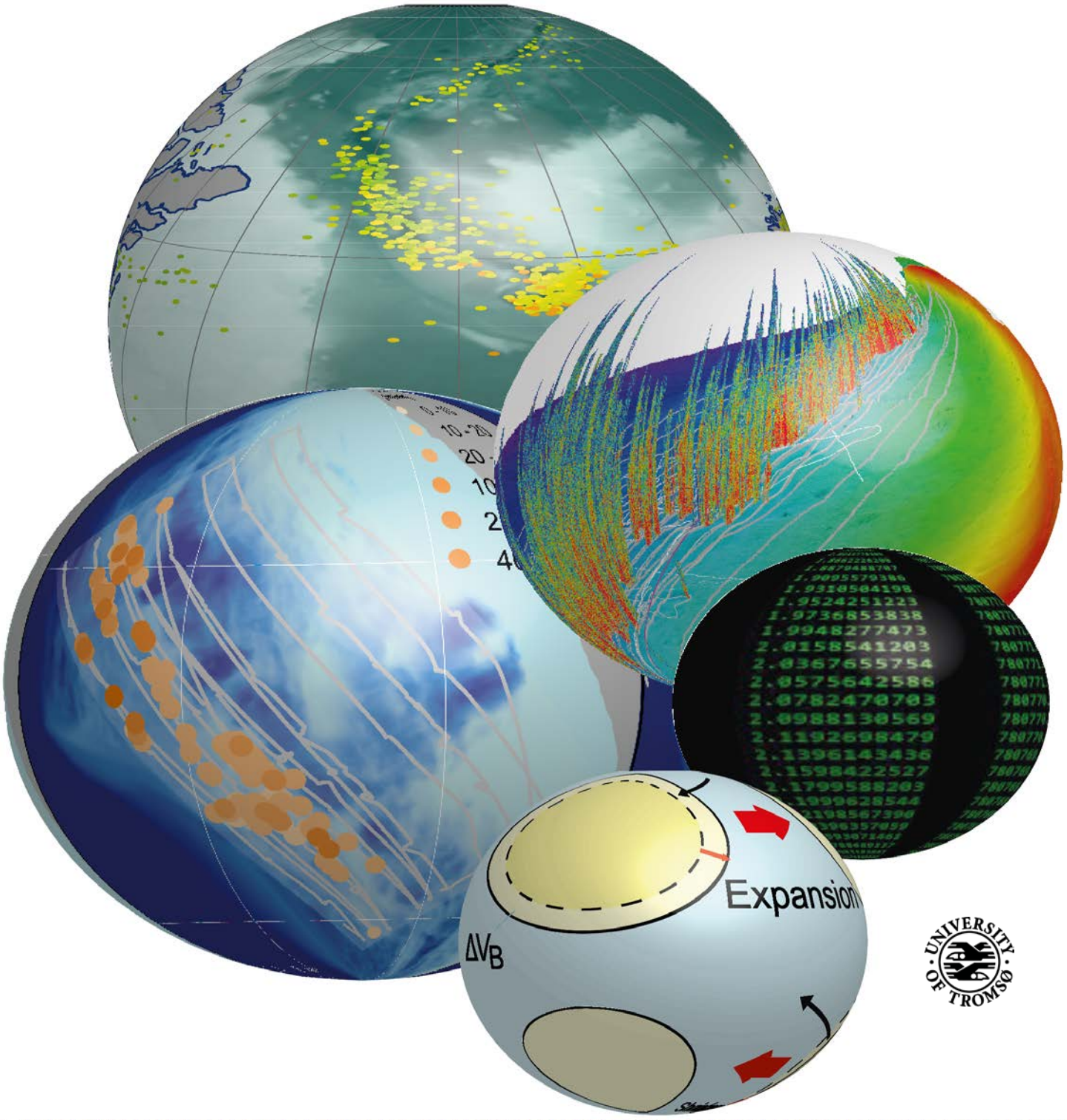

UNIVERSITY OF TROMSØ

Table of Contents

List of Tables

List of Figures

1 Acknowledgements

First, I would like to thank my supervisor Bénédicte Ferré for the support, both personally and scientifically, during the PhD appointment. You always answered my questions quickly and gave relevant and insightful feedback on my work. You made me feel welcome and important in the water column group of CAGE. Anna Silyakova deserves a big thank you for friendly and constructive criticism and helping me to stay focused on the most important tasks. I would like to thank Jens Greinert for inspiring me in the starting phase of the project. Knut Ola Dølven, always enthusiastic and supportive was a big motivator too. The technical staff and administration at the Department of Geosciences (IG) deserves a big thank you for all the support I needed to work with my research questions and take necessary courses and maintaining a very nice work environment. The staff at the IT department of faculty of Science and Technology and at IG. Without the support from the crew on board RV Helmer Hanssen, none of this research would have been possible, so thanks a lot to you all. Finally, I want to thank my family for the support and understanding during lengthy cruises, late night- and weekend work and the few and short vacations.

The research project and PhD appointment was funded by UiT, through its Centre of Excellence funding scheme for CAGE, project number 22359.

2 Preface

This thesis is submitted in partial fulfilment of the requirements for Philosophiae Doctor Degree, PhD, at UiT, the Arctic University of Norway in Tromsø. The PhD appointment started in May 2014 and was funded by UiT, through its Centre of Excellence funding scheme for CAGE, project number 22359 over a period of four years including one year of duty work for the Department of Geology.

The duty work, comprising in total 1655 hours, included participation in the Outreach program Forskningsdagene in 2014; assisting in teaching courses GEO-3182, Marine Geohazards in 2015, 2016, and 2017; GEO-2003, Quaternary Geology in 2015. It also included participation in scientific seagoing expeditions, mainly to areas offshore Svalbard and the Barents Sea. Cruises attended for duty work included CAGE cruises 14-5, 15-3, 15-5, 15-6, 16-2, 16-4, 16-5, 16-7, and 17-1 with RV Helmer Hanssen and PS93.2 with RV Polarstern. Also included was a teaching cruise within the framework of GEO-2010, Marine geology in 2017. The duty work carried out during the cruises included acquisition of data from CTD, ADCP, single beam echosounders and water sampling for CH_4 concentration, nutrients and CDOM. Moreover, the work included plankton net sampling, preparing, retrieving, and sectioning of gravity core sections with subsequent pore water sampling for chemical analysis and preparation of sediment samples for analysis of hydrocarbon gas (C_1-C_5). Assembly, deployment, recovery, disassembly and shipping of CAGE seafloor observatories (K-landers) was also included in the duty work as well as planning, deployment (at 79°4´N 4°7´E, ~2500 m water depth) and recovery of a methane sensor (METS, Franatech) attached to the deep sea lander in the Central Hausgarten (e.g. van Oevelen et al., 2011) in collaboration with Alfred Wegener Institute of Marine Research (AWI).

The thesis at hand comprises a synthesis of a selection of the work conducted during the PhD appointment: an introduction to methane in the water column and working areas with references to

manuscripts considered for the dissertation; a summary of each manuscript; a conclusion and outlook section and the four chosen manuscripts at their current states.

The included manuscripts and the state of their publication processes at the time of the submission of this thesis are detailed in section 3. A co-author declaration, specifying the contribution of all co-authors, is given in section 4. The four manuscripts included in this thesis are:

1. **Variability of acoustically evidenced methane bubble emissions offshore western Svalbard**

2. **Physical controls of dynamics of methane venting from a shallow seep area west of Svalbard.**

3. **A new numerical model for understanding free and dissolved gas progression towards the atmosphere in aquatic methane seepage.**

4. **Insights from underwater high resolution dissolved methane sensing over a known methane seepage site west of Svalbard.**

Apart from the four manuscripts included in this thesis, I also contributed to the following articles during the PhD period:

Lars Arneborg, Pär Jansson, André Staalstrøm, & Göran Broström. 2017. **Tidal Energy Loss, Internal Tide Radiation, and Local Dissipation for Two-Layer Tidal Flow over a Sill.** *Journal of Physical Oceanography, 47(7), pp. 1521-1538.* I contributed to this article with model simulations, analysis of model output and manuscript editing.

Cathrine Lund Myhre, Bénédicte Ferré, Stephen Matthew Platt, Anna Silyakova, Ove Hermansen, Allen Grant, Ignacio Pisso, Norbert Schmidbauer, Andreas Stohl, Jospeh Pitt, Pär Jansson, Jens Greinert, and others. 2016. **Extensive release of methane from Arctic seabed west of Svalbard during summer 2014 does not influence the atmosphere.** *Geophysical Research Letters, 43(9), pp. 4624-4631.* I contributed with 3D image preparation, collection/analysis of discrete dissolved CH_4 samples and with manuscript editing.

Giuliana Panieri, Stefan Bünz, Daniel J. Fornari, Javier Escartin, Pavel Serov, Pär Jansson, Marta E. Torres, Joel E. Johnson, Wei Li Hong, Simone Sauer, Rafael Garcia, Nuno Gracias. 2017. **An integrated view of the methane system in the pockmarks at Vestnesa Ridge, 79° N.** *Marine Geology, 390, pp. 282-300.* I contributed with free gas flow rate calculations based on single beam echosounder data, collection/analysis of water samples and manuscript writing and editing.

Roberto Grilli, Jack Triest, Jérôme Chappellaz, Michel Calzas, Thibault Desbois, Bénédicte Ferré, Christophe Guillerm, Pär Jansson, Loïc Lechevallier, Victor Ledoux, Daniele Romanini. **SUB-OCEAN: subsea dissolved methane measurements using an embedded laser spectrometer technology.** Submitted to *Environmental Science & Technology.* I performed analysis of methane concentrations using gas chromatography and contributed to the manuscript.

Bénédicte Ferré, Pär. Jansson, Manuel Moser, Pavel Serov, Friederike Gründger, Alexey Portnov, Carolyn A. Graves, Christian Berndt, Moritz Lehmann, Helge Niemann. **Cold Seep Hibernation: Seasonal variation of methane emission offshore Svalbard.** In preparation for submission to *Nature Communication.* I contributed with spatial analysis of echosounder data and manuscript preparation.

3 List of papers and co-author contributions

The four manuscripts, included in this thesis and their corresponding publication status at the time of the submission of the thesis are:

1. Mario E. Veloso-Alarcón, Pär Jansson, Marc De Batist, Timothy A. Minshull, Graham K. Westbrook, Heiko Pälike, Stefan Bünz, Ian Wright, Jens Greinert. ***Variability of acoustically evidenced methane bubble emissions offshore western Svalbard.*** Resubmitted to *Geophysical Research Letters*

2. Anna Silyakova, Pär Jansson, Pavel Serov, Bénédicte Ferré, Alexey Pavlov, Tore Hattermann, Carolyn A. Graves, Stephen Matthew Platt, Cathrine Lund Myhre, Friederike Gründger and Helge Niemann. ***Physical controls of dynamics of methane venting from a shallow seep area west of Svalbard.*** Submitted to *Journal of Geophysical Research - Oceans*.

3. Pär Jansson, Bénédicte Ferré, Anna Silyakova, Knut Ola Dølven, Anders Omstedt. ***A new numerical model for understanding free and dissolved gas progression towards the atmosphere in aquatic methane seepage systems.*** Submitted to *Oceanography and Limnology: Methods*.

4. Jack Triest, Pär Jansson, Roberto Grilli, Anna Silyakova, Bénédicte Ferré, Jérôme Chappellaz, Jürgen Mienert. ***Insights from underwater high resolution dissolved methane sensing over a known methane seepage site west of Svalbard.*** In preparation for submission to *Journal of Geophysical Research – Oceans*

3.1 Contributions

Table 1. Author contributions to the manuscripts included in the thesis.

	Paper 1	**Paper 2**	**Paper 3**	**Paper 4**
Concept and idea	MV, JG, MB	AS, BF	PJ, BF	JC, JM, JT, PJ
Study design and methods	MV, PJ	AS, PJ	PJ, BF, AS, AO	JT, PJ
Data gathering and interpretation	MV, PJ*	AS, PJ	PJ, BF	JT, PJ*, RG
Manuscript preparation	MV, PJ*, MB, TM, GW, HP, SB, IW, JG	AS, PJ, PS, BF, AP, TH, CG, SP, CL, FG, HN	PJ, BF, AS, KD, AO	JT, PJ*, RG, AS, BF, JC

** co-corresponding author*

***Authors in Alphabetical order: MB** = Marc De Batist; **SB** = Stefan Bünz; **JC** = Jérôme Chappellaz; **KD** = Knut Ola Dølven; **BF** = Bénédicte Ferré; **CG** = Carolyn Graves; **JG** = Jens Greinert; **RG** = Roberto Grilli; **FG** = Friederike Gründger; **TH** = Tore Hattermann; **PJ** = Pär Jansson; **CLM** = Cathrine Lund Myhre; **JM** = Jürgen Mienert; **TM** = Timothy A. Minshull; **HN** = Helge Niemann; **AO** = Anders Omstedt; **AP** = Alexey Pavlov; **SP** = Stephen Platt; **HP** = Heiko Pälike; **PS** = Pavel Serov; **AS** = Anna Silyakova; **JT** = Jack Triest; **MV** = Mario E. Veloso-Alarcón;*

***GW** = Graham Westbrook; **IW** = Ian Wright*

4 Introduction

One of the major challenges for humankind in the near future is to manage Earth's resources in a responsible way and to maintain an environment suitable for living in. The climate affects us all in daily life and we now experience rapid changes, possibly caused by human activity. It has become increasingly recognized that knowledge of the climate system, its driving forces and feedback mechanisms must be improved in order to help stakeholders, politicians and the general public to take appropriate actions. Climate change is however an extremely complicated subject and multiple processes contribute in ways we can only estimate by developing models. The greenhouse effect, originally suggested by Svante Arrhenius in 1895 (Fleming, 2005), has been a research focus for many decades and the consensus is that gases with warming potential cause heat to be trapped in the atmosphere (Pachauri et al., 2014) and that this is one of the most important topics to study. Methane (CH_4) is a powerful greenhouse gas, estimated to be 32 times more potent than carbon dioxide (CO_2) (Pachauri et al., 2014), contributing to approximately one-sixth of the total warming generated by greenhouse gases in the atmosphere (Kirschke et al., 2013). The oceans play an important role in the global gas budget since the hydrosphere (all oceans, rivers and lakes) stores enormous amounts of dissolved gases. Because gas is constantly exchanged between the atmosphere and the hydrosphere, the oceans can serve as a sink of greenhouse gas but may also contribute with a source to the atmosphere by diffusive equilibration between the dissolved gas in the upper layer of the oceans and the lower atmosphere (Broecker and Peng, 1974; Wanninkhof, 2014).

Moreover, large amounts of CH_4 in aqueous and gaseous form exist in the ocean sediments together with CH_4 in the form of hydrates (e.g. Kvenvolden, 1988; Ruppel and Kessler, 2016), ice-like crystal structures of solid water cages encapsulating non-polar guest molecules. The hydrate structure is stable only in cold environments with high pressure (Sloan, 1998), the so called hydrate stability zone (HSZ). CH_4 hydrates are found on continental margins worldwide and are abundant in the Arctic Ocean (Kvenvolden and Lorenson, 2001). As hydrates dissociate when any of the criteria for their stability is not met (i.e. temperature increases or pressure decreases), it is expected that hydrates located where conditions are close to the hydrate stability limit may dissociate with warming ocean bottom water (Westbrook et al., 2009; Berndt et al., 2014). The effect of dissociating natural gas hydrates would represent a climate feedback mechanism if the resulting CH_4 reached the atmosphere. The Arctic Ocean is currently warming rapidly (Ferré et al., 2012) and concerns have been raised that some CH_4 hydrates will dissociate and that free or dissolved CH_4 gas will seep into the water column and subsequently reach the atmosphere (Shakhova et al., 2010). Numerical modelling by Wallmann et al. (2018) shows that the dominating control mechanism for gas release offshore Svalbard is pressure release after the retreat of the ice-sheet following the last glaciation, rather than ocean anthropogenic effects such as increasing bottom water temperature.

The solubility of CH_4 is reduced at lower pressure and higher temperature. This could, if the concentration of dissolved CH_4 in pore water is high, cause gas to come out of solution (exsolve) and spontaneously form bubbles. Römer et al. (2016) showed that gas bubble release increased during decreasing tidal pressure at a site west of Vancouver. Flares were observed to recur at tidal frequency east of New Zealand (Linke et al., 2010). Thus, it is expected that pressure changes on short and long time scales is a controlling factor for the intensity of benthic gas release.

By geochemical modelling, Fischer et al. (2013) found a relation between a major earthquake in 1945 and increased upwards flux of CH_4, lasting for several decades in the area offshore Pakistan. As our study site (see section “Study Area”) is located in a seismically active zone (Plaza – Faverola et al., 2015) with frequent earthquakes in the vicinity (International Seismological Centre 2014), it may be expected that the seepage intensity is influenced by seismic activity.

It is imperative to understand these, and possibly other, controlling mechanisms on methane seepage activity. In Paper 1, we presented a conceptual model, bearing in mind the proposed controlling mechanisms, and we compared their variations with free gas flow rates inferred from echosounder data collected during 11 cruises and a time span of 8 years.

The fate of CH_4, bubbling from the seafloor, depends on physical oceanographic conditions, ocean-atmosphere interaction, and biochemical processes in the water column. Ocean currents carry dissolved methane away from the local bubble sources and therefore play a major role in the horizontal distribution of dissolved CH_4, together with mixing induced by horizontal eddies and diffusion. In Paper 2, we investigate the relation between seepage activity, subsequent release to the atmosphere, oceanographic conditions, and the observed resulting distribution of dissolved CH_4.

The vertical distribution of the bubble-mediated CH_4 is governed by the interaction of the bubbles with the ambient conditions. While bubbles rise through the water column, gas of all present species may dissolve or exsolve depending on whether the ambient concentration is lower or higher than the equilibrium concentration of the corresponding gas inside the bubble. The rate of gas transfer across the bubble rims depends on the magnitude of the concentration gradient, the gas diffusivity, the bubble rising speed, the local turbulence, the temperature and the salinity (e.g. Leifer and Patro, 2002; McGinnis et al., 2006). Therefore, the bubbles affect and are affected by the ambient conditions and must be understood simultaneously with the local water column conditions. In Paper 3, a new numerical model was presented, that resolves the dynamics between bubble- and dissolved gas. The model also included aerobic oxidation, which occurs when methanotrophic bacteria are present in the water column (Reeburgh, 2007).

At a site where the HSZ pinches out at the seafloor, it has been speculated that observed CH_4 bubbles derive from dissociating hydrates (Westbrook et al., 2009; Berndt et al., 2014). In Paper 4, we investigate this site, using the gas flow rate estimation method from Paper 1 together with the prediction of vertical CH_4 distribution from the process-based model in Paper 3.

5 Study area

During the period of this PhD project, several CAGE research cruises have visited at least five prominent seepage areas west and northwest of Prins Karls Forland (PKF) and the Barents Sea, as indicated by yellow stars in Figure 1.

In the Barents Sea, CAGE investigates at least three areas of seepage activity. Intense bubbling occurs from pingo-like features at 370 – 390 mbsl, south of Spitsbergen (Serov et al., 2017). At the so called Crater Area (330 – 360 mbsl), located in the Bjørnøy through, seepage exist from crater-like features, postulated to derive from blowout of free gas and hydrates as hydrates dissociated due to the pressure release after the last glacial period (Andreassen et al., 2017). Pingo like features with gas leakage have also been observed in the Maud Basin.

Persistent CH_4 seepage exist at Vestnesa Ridge (e.g. Panieri et al., 2017), near the spreading ridge system (Molloy Transform Fault; Spitsbergen Transform Fault; Molloy Ridge; Knipovich Ridge). The ridge area (~1200 mbsl) has been monitored by the Institute of Geoscience (IG) of The Arctic University of Norway, Tromsø, and CAGE since the discovery of CH_4 seepage from pockmarks in 2008 (Hustoft et al., 2009; Bünz et al., 2012). Seismic studies show that the Vestnesa Ridge sediments host hydrates and trapped gaseous CH_4, susceptible to release where and when fractures occur in the sediments due to tectonic stress (Plaza – Faverola et al., 2015).).

The main study area for this thesis was the location offshore PKF, where many gas flares have been observed. The seepage here can be divided into three areas, comprising the shallow shelf (~50 – 150 m water depth), the shelf break (~250 m), and the continental slope (~400 m). In Paper 1, we used data from 11 cruises which covered all three areas (Figure 1 and Table SI1 in Paper 1). In Paper 2, we focus on the shallow shelf, using three datasets from consecutive years, covering the same area. The seepage at the slope was examined with high resolution methane sensing, described in Paper 4 and was included as a case study for the model described in Paper 3.

Despite substantial research efforts, the origins and controls of gas seepage in this area are still not completely elucidated. The shallow shelf (~50 – 150 mbsl) is too shallow for gas hydrates to exist near the seafloor and it is believed that the seepage here presently occurs as a consequence of decreased pressure after the ice sheet retreated, following the last ice age (Portnov et al., 2016). This was also the control mechanism suggested for the crater Area in the Barents Sea.

At the slope (~ 400 mbsl), seepage has been associated with gas hydrates, since the conditions (high pressure, low temperature) for their stability are met. More precisely, the seafloor conditions here are at the limit of the stability for CH_4 hydrates and so short- and long-term temperature variations pushes the stability zone downslope during warm periods and upslope during cold. This, at least in theory, triggers dissociation of hydrates and varying CH_4 emissions. However, no hydrates have been recovered to date (Riedel et al., 2018), and the existence of hydrates has not been proven by seismic studies (Rajan et al., 2012). On the other hand, Rajan et al. (2012) did not rule out the possibility that hydrates are present and Wallmann et al. (2018) found evidence of hydrate dissociation in the pore water composition. The authors consequently suggested that temporal hydrate formation and dissociation controls CH_4 migration pathways. Such dynamic blockings would explain seasonality of benthic free gas seepage intensity (Ferré et al., submitted to *Nature Communications*).

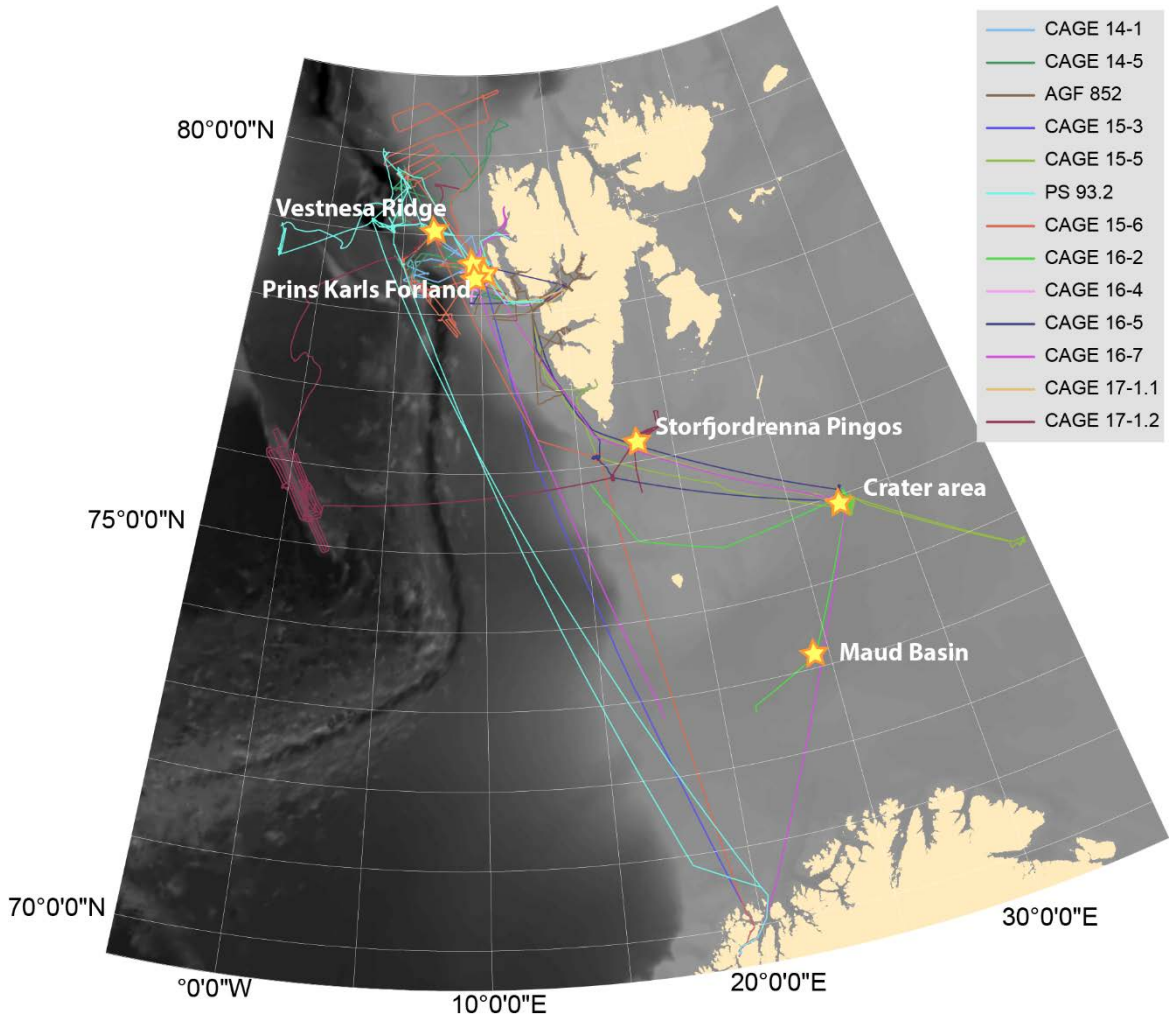

Figure 1. Overview of cruises and investigated methane seepage areas. Stars indicate observed methane seepage areas and lines indicate vessel cruise tracks of attended cruises. Place names and water currents are detailed in paper 1, Figure 1.

It would also explain the findings in Paper 1, namely that gas release intensity varies inversely between the slope (~400 mbsl) and the shelf break (~250 mbsl). We suggested that the two areas are connected through sub seafloor gas migration pathways and that seasonal blocking and opening of the pathways control the seepage intensity at the two locations. Seismic evidence of permeable and impermeable strata, providing such gas migration pathways, was presented by Rajan et al. (2012).

The fate of the bubble-mediated CH_4 emissions largely depends on water column properties and movement by currents (Figure 1, paper 1). The study area hydrography is mainly controlled by the West Spitsbergen Current (WSC), which carries relatively warm and saline Atlantic Water (T>3.0°C in the warm season; S>34.65 PSU; σ <27.92 kg m^{-3} (Cottier et al., 2005)). In addition, the Coastal Current (CC), the extension of the East Spitsbergen Current (ESC), carries colder and less saline water along the western Spitsbergen coast. The front between WSC and CC meanders longitudinally across the slope (Steinle et al., 2015) and is subject to instabilities, and so eddies are ubiquitous on the slope and shelf (Appen et al., 2016). The interplay between the two currents, each carrying different water

masses, results in variable water properties on the shelf, which are additionally affected by local processes such as river run-off and cooling/ heating from the atmosphere.

6 Methods

6.1 Detection and quantification of benthic gas emissions

Owing to the contrasting acoustic properties of free gas and water, bubbles in the water column can be detected by acoustic methods (e.g. Medwin and Clay, 1997; Nikolovska et al., 2008; Weber et al., 2014). The EK60 split-beam echosounder was developed for the fishing industry for quantification and identification of fish stocks (e.g. MacLennan, 1990) but has frequently been used to detect free gas bubbles in the water column (e.g. Haeckel et al., 2004; Maksimov and Sosedko, 2005; Greinert et al., 2006). So-called flares (acoustic signatures of bubble streams in the water column, seen in echograms) can be extracted from echosounder data and easily visualized with the Fledermaus Midwater module (www.qps.nl/display/fledermaus/). This makes mapping of gas seepage relatively simple as shown in Figure 2, which shows flares from surveys conducted in 2010, 2013 and 2015 over the slope seepage area west of PKF.

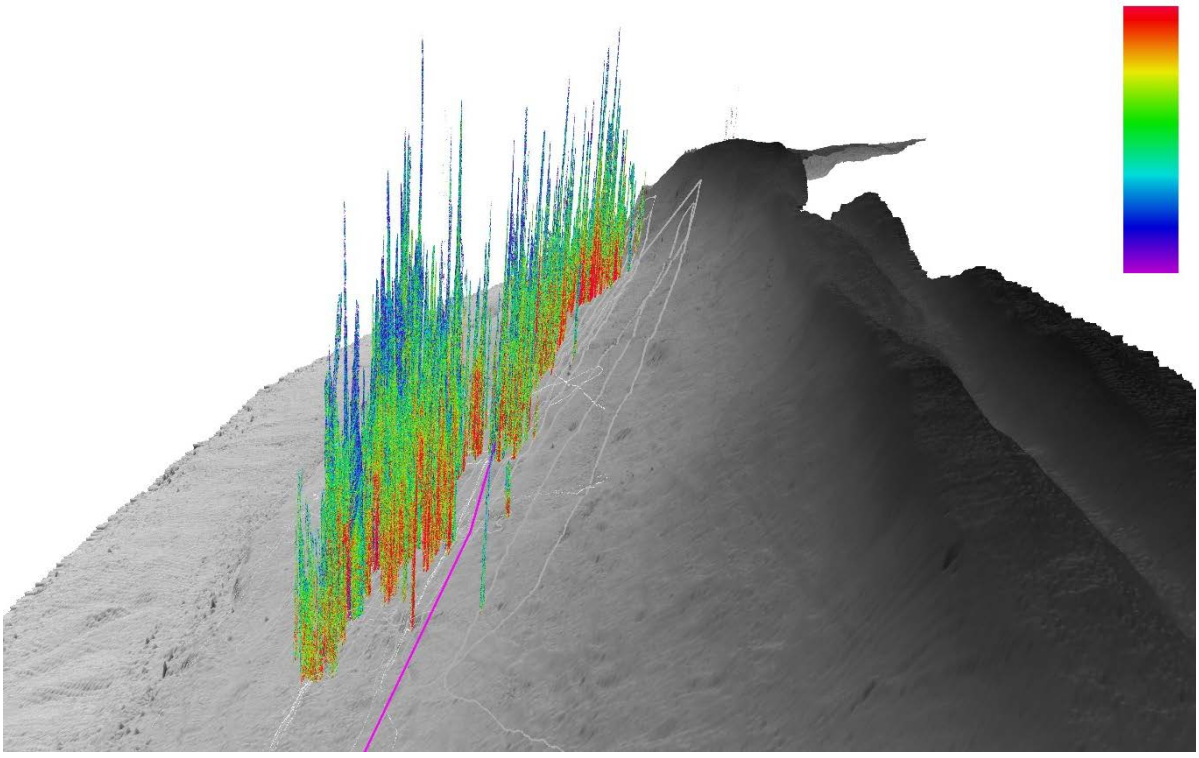

Figure 2. 3D visualization of free gas in the water column detected by echosounder View of free gas in the water column, produced with the Fledermaus QPS software. The echosounder data displayed here stem from cruises in 2010, 2013, and 2015 on the ~400m seepage site west of PKF. Coloured scale indicates the target strength (TS, dB) of the acoustic backscatter. Ship tracks are seen as grey lines and a modelled outcrop of the gas hydrate stability is shown as a purple line.

The mapping allows for comparison with seafloor features such as pockmarks, faults and chimneys and possibly cold-water coral reefs (Hovland and Thomsen, 1997).

The amount of free gas in the water column can also be acoustically quantified with calibrated single-beam echosounders. Provided knowledge of pressure, gas composition, temperature, size and rising speed of the detected bubbles, flow rates can be estimated (Veloso et al., 2015) and repeated echosounder surveys may elucidate on the spatial and temporal variability of free gas emissions.

For our analysis described in Paper 1, echosounder data was collected during eleven cruises using split-beam echosounders mounted on research vessels RV Helmer Hanssen (UiT, The Arctic University of Norway) and RV James Clark Ross (British Antarctic Survey). The split beam echosounder SIMRAD EK60 was operated at 38 kHz, which has been the preferred frequency for detecting bubbles in the water column (e.g. Artemov et al., 2007; Sauter et al., 2006; Veloso et al., 2015).

Estimation of free gas flow rates requires knowledge of water properties, such as temperature, salinity, and pressure. Hence, we gathered oceanographic data for the calculations, described in the section *Oceanographic influence* and seen in Figure 7.

Echosounder data was analysed with the Fledermaus Midwater software and acoustic flares were identified and separated from other scattering objects such as fish, seafloor, strong density gradients, and interference from other acoustic instruments (Figure 3). Subsequently, free gas flowrates were calculated with the FlareHunter software and the FlareFlow Module embedded in the same software bundle (Veloso et al., 2015).

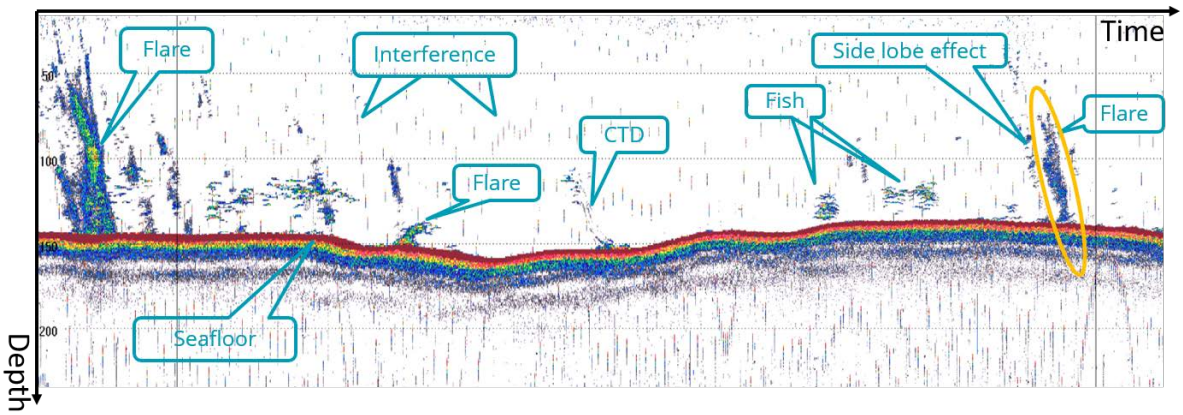

Figure 3. Typical echogram showing flares (An example is highlighted by the yellow oval) and other scattering objects in the water column as indicated by the callouts.

We distinguish bubble streams (flares) from other scattering objects by visual inspection of the echograms (Figure 3). Flares typically extend almost vertically from the seafloor and have a larger vertical than horizontal extent, whereas fish schools are often seen in midwater and do not extend vertically. The seafloor is easily detected as it fills the echosounder beam completely and therefore returns a large fraction of the acoustic signal. Interference from other instruments, typically acoustic Doppler current profilers (ADCPs), multibeam echosounders (MBEs) and frequency-modulated sounders (CHIRPs), is easily distinguished as it occurs in single pings and regular patterns (Figure 3).

In paper 2, we reported on free gas flow rates from echosounder data collected during three research cruises and three consecutive years (2014 – 2016), which covered the same area west of PKF. The surveyed area was approximately 400 km^2 with water depths varying between 50 and 150 m and the ship tracks were 300 – 430 km, resulting in beam coverage between 3.8 and 5.5 km^2.

We calculated echosounder/Flarehunter derived flow rates from a cruise to the slope area west of PKF in October 2015. In paper 3, a new numerical marine 2-phase gas model in one dimension (M2PG1) was presented, for which we used the acquired flow rate data to force case study simulations.

In Paper 4 we used the mapped and calculated flow rates in conjunction with results from M2PG1 to force a 2-dimensional model, and as flux approximation to an analytical steady state calculation.

6.2 Dissolved CH_4

Dissolved CH_4 can be measured by direct sampling of small water quantities and subsequent headspace gas chromatography (GC). This is common praxis in the research field of marine methane. Alternatively, concentrations can be measured using in-situ deployed sensors.

6.2.1 Discrete sampling

Measurements of dissolved CH_4 can be used to map the distribution of CH_4 in the water column in three dimensions. The method is however, time consuming and gives sparse data. Typically, the water is sampled at discrete sampling depths at each sampling station and the possible vertical resolution depends on the number of Niskin bottles available on the rosette. In oceanographic surveys, it is typical to sample seawater in a resolution of kilometres to hundreds of kilometres. However, for the purpose of mapping CH_4 emanating from the seafloor it is beneficial to sample denser grids. Sampling with Niskin Bottles attached to a rosette is standard procedure and subsequent subsampling into serum bottles allow for various chemical analysis. Dissolved CH_4 can be analysed after introduction of headspace gas with zero or known CH_4 content. The headspace is allowed to equilibrate with the water sample and is further analysed by gas chromatography (GC) with a flame ionization detector. The method is detailed in Paper 2 and is similar to the method presented in Magen et al. (2014). In Paper 2, we present dissolved CH_4 data acquired from 64 stations from which we sampled during three surveys in three consecutive years 2014 – 2016. In Paper 3, discrete sampling of CH_4 was used to assess the agreement between measurements and model results. The vertical profiles obtained by discrete sampling and model results were also used as input to a 2-dimensional model in Paper 4.

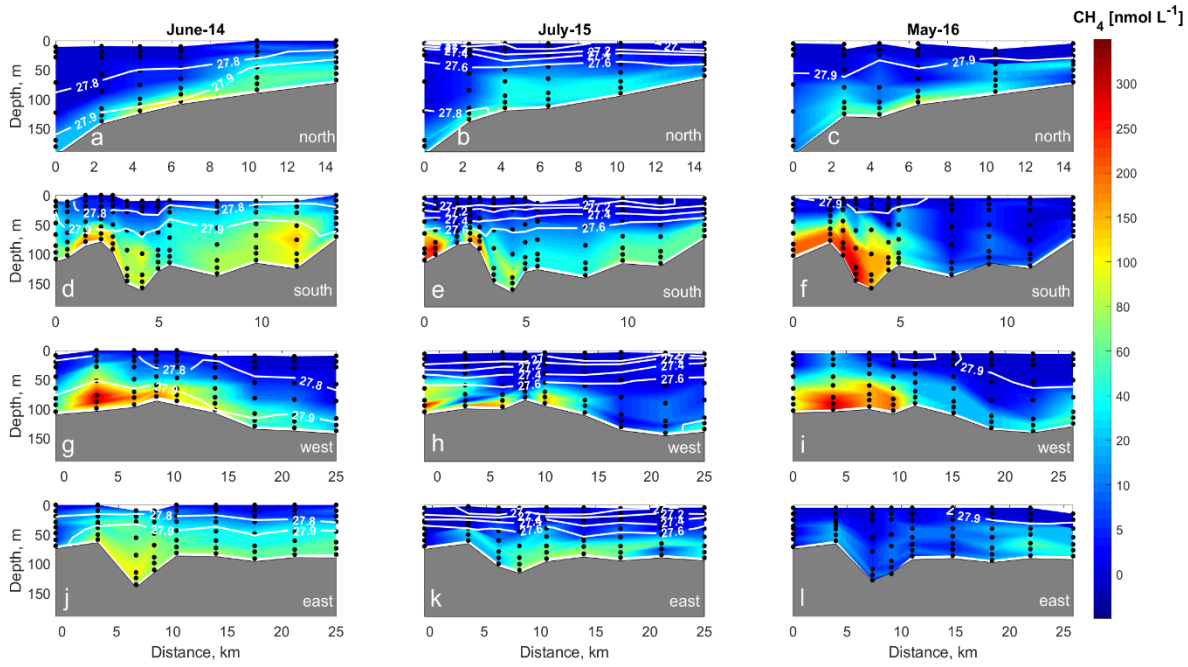

Figure 4. Example of CH_4 concentrations acquired from discrete water sampling. Coloured contours indicate data interpolated between discrete sample depths (black dots). The white lines indicate isolines of density anomaly (kg m^{-3}).

6.2.2 High-resolution measurements

During a three-day survey (October 21 – 23) offshore Svalbard in October 2015, we performed high-resolution CH_4 measurements with a newly developed Membrane Inlet Laser Spectrometer (MILS) (Grilli et al., submitted to *Environmental Science & Technology*) towed behind the research vessel. Sampling with the MILS at a frequency of 1 Hz allowed for unprecedented spatial resolution during both vertical casts and horizontal towing at depths down to 400 mbsl. In Paper 4, the data from the instrument was compared with echograms and showed high values and strong gradients close to gas seepage locations (Figure 6). It resolved the CH_4 concentrations much better than a commonly used reference sensor.

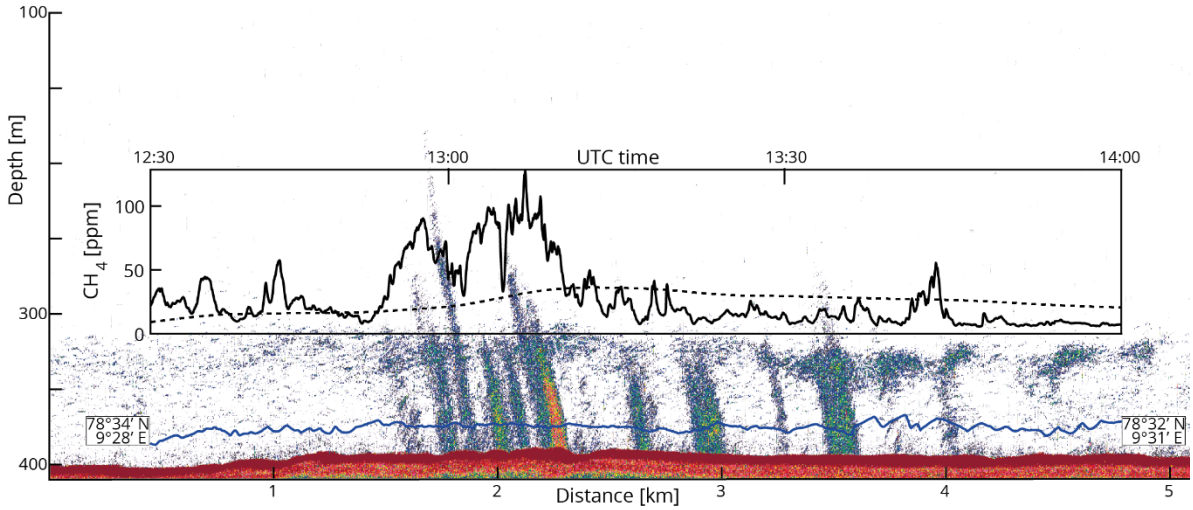

Figure 5. Example data from the towed instrument campaign during the CAGE 15-6 cruise. The top inset panel shows temperature- (red) and salinity- (black) anomaly. The lower inset panel shows MILS data (solid line) and reference sensor data (dashed line). The blue line indicates instrument depth and the background shows backscatter intensity (TS values (dB).

We assessed the agreement between discrete and continuous CH_4 data in Paper 4.

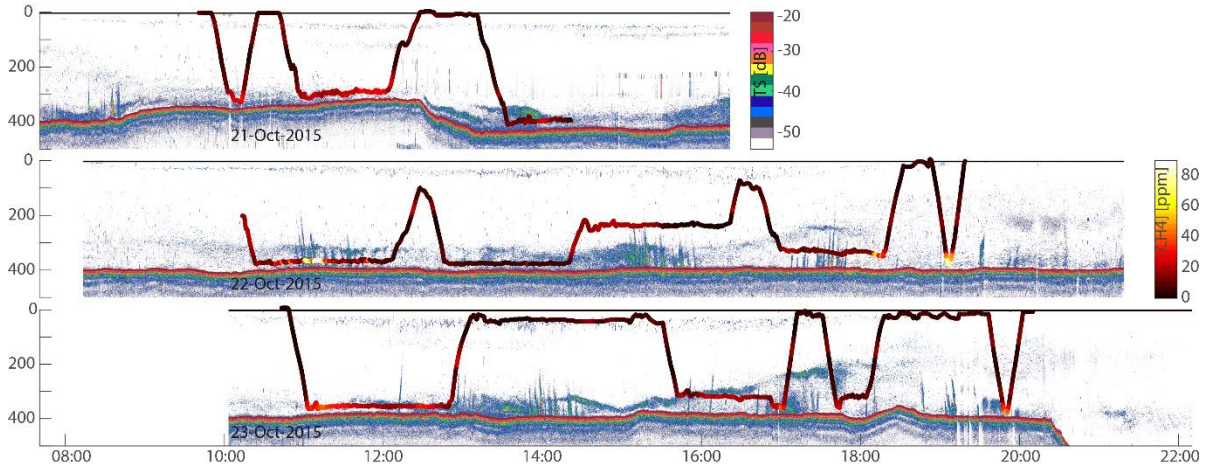

Figure 6. High-resolution measurements with MILS superimposed on echosounder data. The position of the dark red to light yellow track starting around 10 AM each day represents the depth of the MILS sensor and the colour indicates CH_4 mixing ratios measured by the MILS. The background represents the acoustic target Strength (TS), acquired with the echosounder, with a minimum cut-off at -55 dB. High values (red) indicate large abundance of CH_4 bubbles in the water column. The time axis represents local time (2 hours ahead of UTC, for comparison with Figure 5)

6.3 Oceanographic influence

In the framework of working with free and dissolved gas in seawater, it is imperative to know the water properties. In our studies, the water properties influence; a) the free gas quantification method (Flarehunter) because they affect the bubbles' acoustic properties and their rising speeds; b) the process based modelling because they influence the gas dynamics though gas solubility, bubble rising speed and gas transfer efficiency across the bubble rims; c) the control volume model and 2D model are affected through the current velocity and eddy diffusivity.

For the quantification of benthic CH_4 emissions with Flarehunter, conveyed in Paper 1 – 4, knowledge of pressure, salinity, and temperature is necessary. For that purpose, we used CTD (Conductivity, Temperature, and Depth) profiles from hydrocasts performed during the corresponding cruises, and where no such data was available, we downloaded relevant salinity, temperature, and pressure data from the World Ocean Database, managed by the National Oceanographic Data Center: https://www.nodc.noaa.gov/cgi-in/OC5/NPclimatology/arctic.pl

Profiles of seawater density and sound velocity were calculated from the pressure, temperature, salinity profiles, using the GSW Oceanographic Toolbox (McDougall and Barker, 2011), as seen in Figure 7.

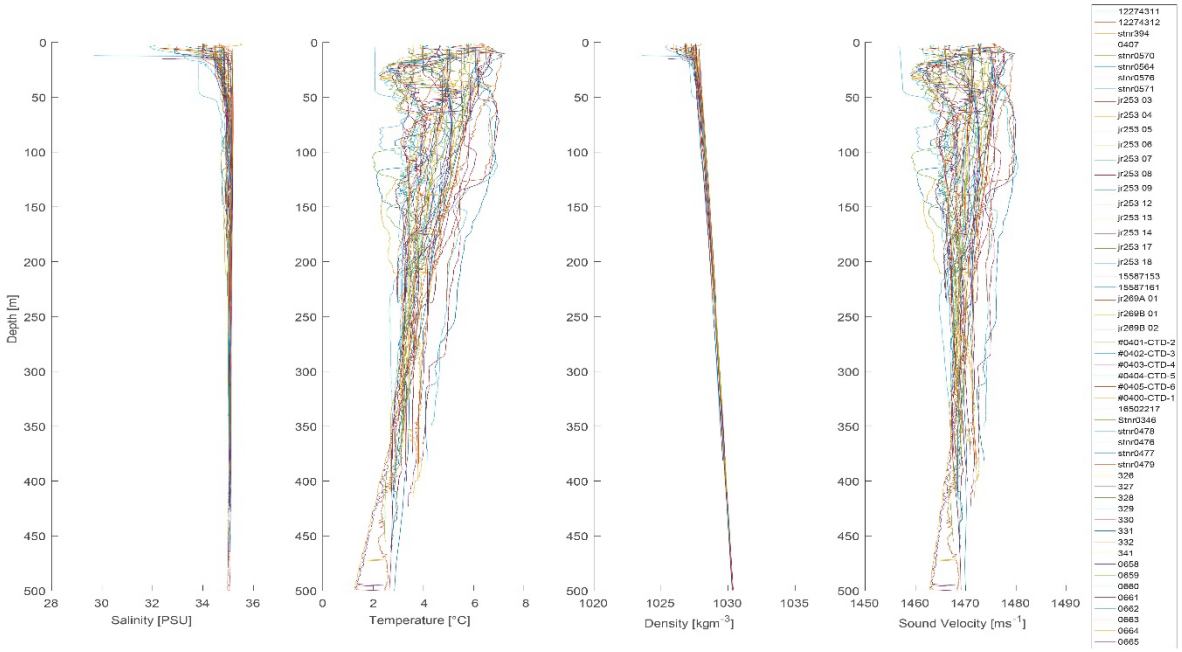

Figure 7. Water properties used for flow rate calculations. Most of the data was acquired during cruises and when not available (profiles 12274311, 12274312 and 165502217), downloaded from the World Ocean Database.

We further used the acquired bottom water temperatures for comparison with temporal seepage activity changes as described in Paper 1.

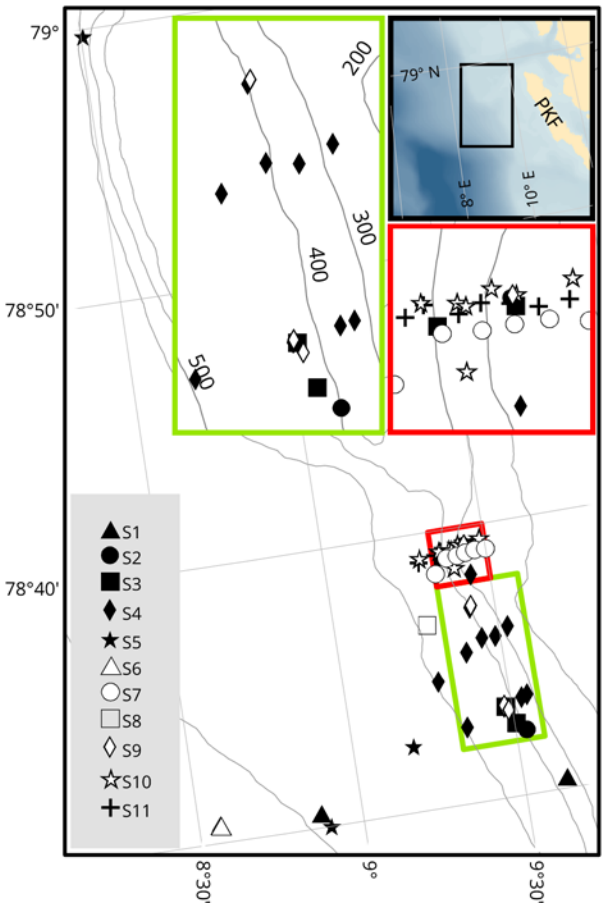

Figure 8. Map of CTD-stations used for flow rate calculations in Paper 1. The shelf break area is boxed with red lines and the slope area is boxed with green lines. Legend indicates which survey the CTD cast refers to. The inset coloured frames show zooms of the two areas and the black framed map shows the location of the sites offshore PKF. Data from the individual CTD casts are shown in Figure 7.

In Paper 2, we show some of the variability in water properties on the shelf based on three surveys repeating a CTD cast grid consisting of 64 stations. To understand the fate of CH_4 coming from seepage on the shelf, we used an existing ocean circulation model (Svalbard 800) (Hattermann et al., 2016) and performed synthetic neutrally buoyant drifter experiments, where the drifters represented inert CH_4.

We estimated the WSC velocity based on the inclination of flares in Paper 4, and subsequently incorporated it in the 2-dimensional model, the control volume model, and the analytical solution to the steady-state CH_4-budget model, all described in section 6.4 (this thesis) and in Paper 4.

6.4 Modelling free and dissolved gas

Three types of models were constructed for Paper 3 and Paper 4.

Paper 3 presents a newly developed numerical model resolving the exchange of gas over bubble rims while bubbles rise through the water column. Bubble shape- and size-changing, aerobic oxidation of dissolved methane and eventual release of gas to the atmosphere is predicted by the model called M2PG1 (Marine 2-Phase Gas model in 1 dimension). M2PG1 is fully Eulerian with multi-sized bubbles containing gas of several species and it accounts for non-ideal gas behaviour and includes the latest parameterizations of solubility, diffusivity, and molar volumes available in the literature. M2PG1 was developed in order to predict the vertical distribution of dissolved CH_4 resulting from the release of bubbles from the seafloor and along vertical bubble trajectories. Although it was originally intended to resolve methane dynamics, it simultaneously models other included gas species (N_2, O_2, CO_2 and Ar) allowing for numerical experiments with gas bubbles containing any or all of these gas species. Paper 3 describes the numerical construction of the model, provides a sensitivity analysis and compares the model output with observations made at the slope offshore PKF, which is known for intensive CH_4 seepage offshore Svalbard (e.g. Berndt et al., 2014; Westbrook et al., 2008).

A 4.5 km long and 400 m high 2-dimensional model was constructed along the slope offshore Svalbard, at ~38.5°N, 9.3°E, which corresponded to line 3, described in Paper 4. The model resolved horizontal diffusion of CH_4 across the domain and advection with water currents. It was run to steady state and thereafter compared with high-resolution (MILS) CH_4 data. We calculated flow rates from the echosounder data with Flarehunter and its bundled Flare Flow Module and constructed a map with quantified sources of bubble-mediated CH4. The mapped flare positions and flow rates were used as input to the new 2-d model. The vertical distribution of the bubble-mediated CH_4, predicted by the M2PG1 Case study, described in Paper 3, was used to distribute the CH_4 source vertically in the 2-d domain. Different diffusion coefficients were tried and the best model agreement with MILS data was achieved with a 2 m^2s^{-1} diffusion coefficient. Paper 4 describes the construction of the 2D model and compares its output with the high-resolution CH_4 measurements.

An analytical solution to a steady-state model was derived in order to comprehend elevated mean CH_4 concentrations in a defined water volume. We assumed that the CH_4 concentration within the volume (V) was affected by inflow (in the x-direction) of seawater carrying background concentration of CH_4 and outflow of water carrying momentary CH_4 concentration. Further alteration of the CH_4 concentration in the volume was provided from bubble sources and diffusion (in the y-direction). The equation for the temporal concentration change in the volume was thus:

$$\frac{dC}{dt} = \frac{Q_{IN} \times C_B}{V} - \frac{Q_{OUT} \times C}{V} + \frac{F_{CH4}}{V} + k\frac{\partial^2 C}{\partial y^2},$$

Where C and C_B are the temporal and background concentrations respectively and k is the horizontal mixing coefficient. This equation is a first order differential, and realizing that the second gradient can be discretized $\left(\frac{\partial^2 C}{\partial y^2} = \frac{2(C_B - C)}{(\Delta y)^2}\right)$, one can calculate the steady state concentration:

$$C_{t=\infty} = \frac{\left(\frac{Q_{IN} \times C_B}{V} + \frac{F_{CH_4}}{V} + \frac{2k \times C_B}{(\Delta y)^2}\right)}{\frac{Q_{OUT}}{V} + \frac{2k}{(\Delta y)^2}}$$

The results from the analytical steady state model are presented in Paper 4.

7 Summary of manuscripts

7.1 Paper 1

Mario E. Veloso-Alarcón, Pär Jansson, Marc De Batist, Timothy A. Minshull, Graham K. Westbrook, Heiko Pälike, Stefan Bünz, Ian Wright, Jens Greinert, ***Variability of acoustically evidenced methane bubble emissions offshore western Svalbard.*** Resubmitted to Geophysical research letters

In this study, we examined the variability of free gas emission from the seafloor to the water column in an area west of Svalbard (Figure 1). We processed echosounder data from eleven surveys conducted between 2008 and 2014. For the first time, free gas emission inferred from an acoustic method over a large area has been collected over a longer period. Flares, the acoustic signature of gas bubbles in the water column, were identified mostly in three distinct areas offshore Svalbard on the continental shelf (water depth ~70-150 m), shelf break (depth ~250 m) and on the slope (depth ~400 m).

We estimated that the three prominent seepage areas (Figure 9) emit in total 2900–4500 t CH_4 y^{-1}. Because the beam width of the single beam echosounder is narrow, and ship-tracks are never identical between surveys, it is clear that data from different surveys never have identical coverage. It was thus necessary to develop a comparison method only taking into account the small areas that were covered by the echosounder beam several times. This so-called common area comparison (CAC) showed that flow rates from two adjacent seepage areas, the Shelf break and Slope, varied inversely with time, suggesting that the two areas are interconnected by sub-seafloor features (permeable layers) where the gas can migrate horizontally. No trend toward increased seepage could be inferred from the analysis, as would have been expected from long-term bottom water warming (Ferré et al., 2012). We attempted to establish a correlation between free gas flow rates and pressure changes induced by tides (Boles et al., 2001) and compared modelled sea surface heights (Egbert and Erofeeva, 2002) with calculated flowrates but we found only a small correlation. A similar analysis comparing earthquake data with the backscatter intensity showed no correlation. We found no evidence for migration of seep locations over time, as would have been expected from bottom water warming and subsequent offshore migration of the Methane hydrate stability limit.

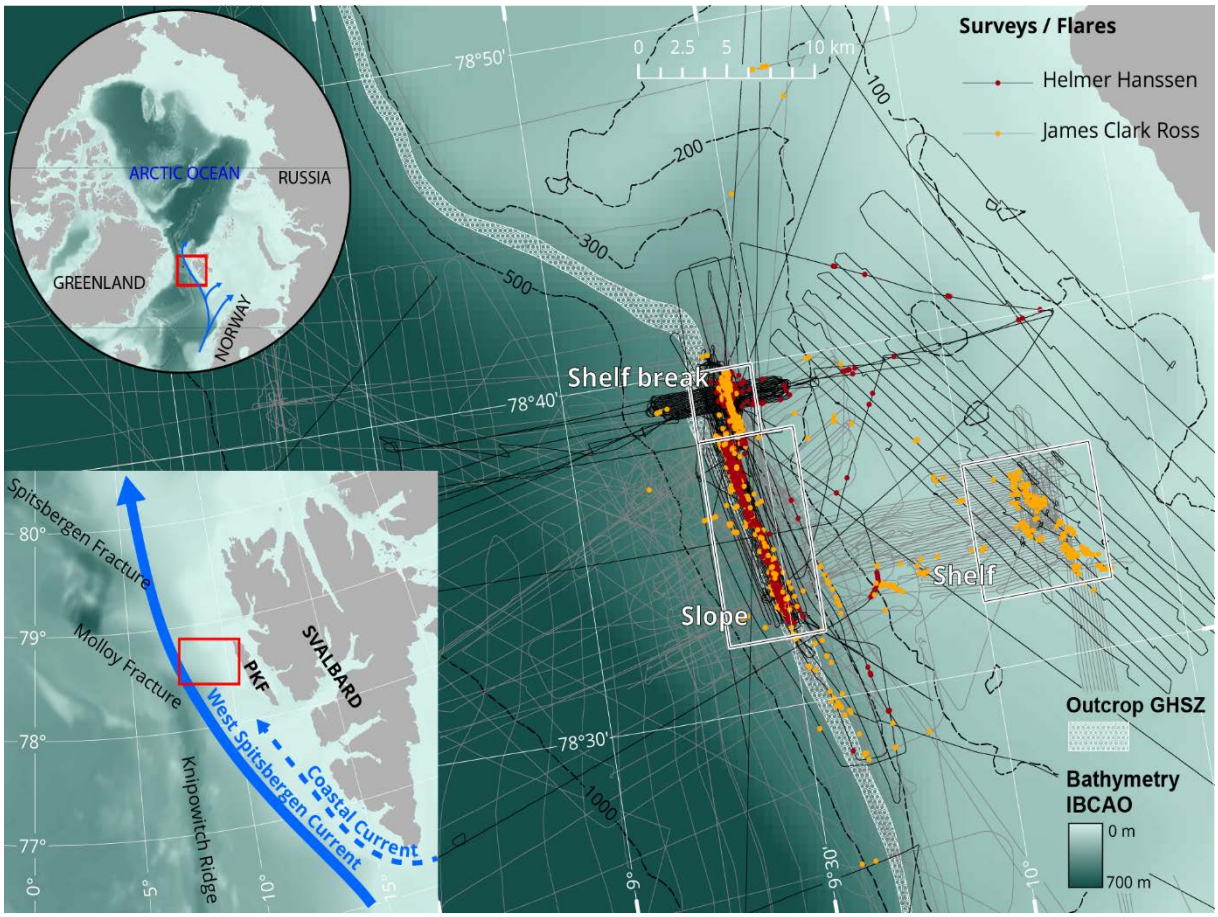

Figure 9. The study site and defined seepage areas. Black lines and red dots indicate ship tracks and flare observations by RV Helmer Hanssen. Grey lines and orange dots represent RV James Clark Ross tracks and flares observations. The outcrop of the gas hydrate stability zone (GHSZ), showed as a hex pattern was inferred from the migration between 360 and 410 m. water depth, suggested by Berndt et al. (2014).

The paper was well received by the editor but two reviewers requested restructuring and a revised manuscript was submitted. After the re-submission, both reviewers were satisfied but a third reviewer suggested further changes. We are currently working on a third version of the manuscript, which should be submitted in October 2018.

7.2 Paper 2

Anna Silyakova, Pär Jansson, Pavel Serov, Bénédicte Ferré, Alexey Pavlov, Tore Hattermann, Carolyn A. Graves, Stephen Matthew Platt, Cathrine Lund Myhre, Friederike Gründger and Helge Niemann. ***Physical controls of dynamics of methane venting from a shallow seep area west of Svalbard.*** Submitted to JGR Oceans.

The area offshore Svalbard has been well studied since methane bubble streams were discovered on the shallow shelf, the shelf break, and the continental slope. We present data from three seagoing research expeditions, repeatedly covering the same area of approximately 400 km^2 with water depths ranging between 50 and 150 m. We performed 64 hydrocasts during each expedition, collecting water samples and CTD data (salinity, temperature, depth). The collected water samples were later analysed for methane concentration using headspace gas chromatography.

We also acquired echosounder data, using the shipborne EK60 echosounder, which we analysed for acoustic gas flares (signatures of bubble streams emanating from the seafloor) with the FlareHunter software (Veloso et al., 2015). In order to obtain unbiased CH_4 flow rate estimates for each cruise, the acquired flow rates were upscaled using ArcGIS in a manner so that the different lengths of the ship tracks and echosounder beam coverage did not influence the resulting area-flow rates. The upscaling method was described in the SI of Paper 2. Figure 9 shows the flare positions and the upscaled CH_4 flow rates.

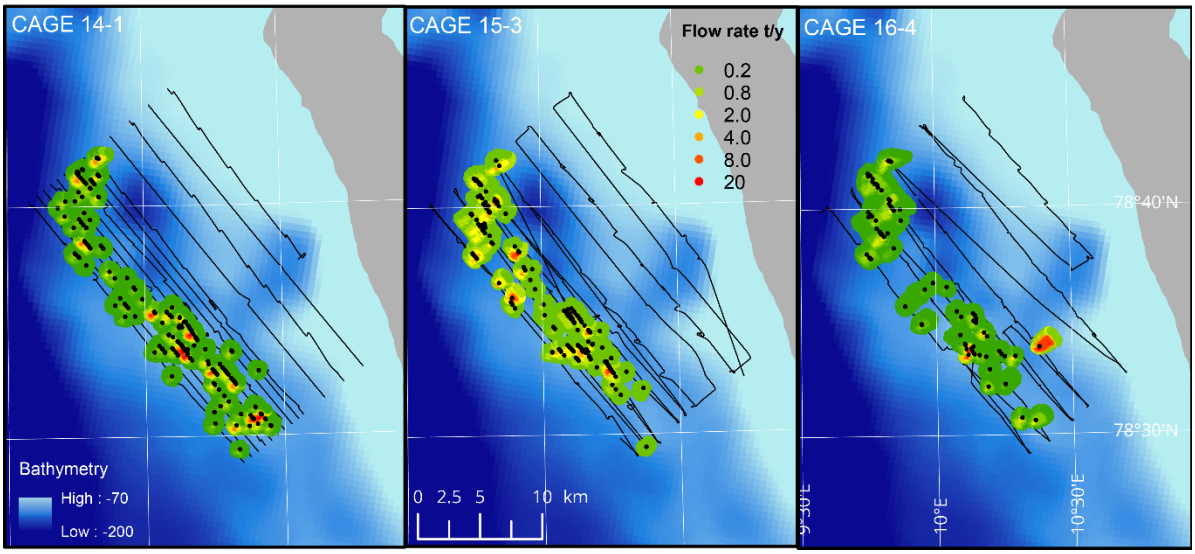

Figure 10. Upscaled flow rates from cruises in June-14, July-15 and May-16. Observed flares (point sources) are shown as black dots. Colour scale from green to red indicates the upscaled flow rates on a 100 x 100 m grid.

We found that the upscaled flow rates were largest in June 2014, with 3774 t y^{-1} and that this coincided with high methane content in a defined water volume. In July 2015, the flow rates were slightly lower (3004 t y^{-1}) and correspondingly, the weighted average methane content in the same volume were lower. In May 2016, both the flow rates and methane content were at the lowest level at 2356 t y^{-1}.

The bubble-mediated dissolved CH_4 measured with discrete sampling and headspace GC, did not reach high into the water column during any of the surveys. The occurrence of water density

stratification in July-15 and the lack thereof in June 2014 and May 2016 did not affect the vertical extent of the aqueous CH_4, which we attributed to fast dissolution of bubbles near the seafloor and inefficient diapycnal mixing also when stratification was weak.

We analysed numerical ocean-circulation model data, and performed synthetic neutral buoyancy particle drifter experiments, comparing with the observed CH_4 distributions. The numerical model showed seasonal efficiency of particle dispersion. A large area was particle covered in January to May, whereas a smaller area of high particle concentrations was modelled for the summer months. These modelling results suggested that dissolved CH_4 is less dispersed during summer. Key to how this correlates with our findings is understanding the temporal dispersion pattern: In May 2016, we observed high concentrations in a limited area around the flares wand otherwise low concentrations. This is predicted by the model which predicts intense dispersion in spring. Efficient dispersion was taking place while CH_4 was emitted at a few places only, explaining the observed CH_4 distribution.

Equilibration of CH_4 with the atmosphere was calculated, using the surface-water CH_4 concentration, atmospheric mixing ratio, and wind speeds. During our surveys, the diffusive CH_4-flux to the atmosphere was small with the exception of an area in the south corner of the defined area in May 2016, where some enhanced CH_4 was observed near the surface.

In summary, the content of CH_4 in the water column was related to the magnitude of the bubble seepage and the distribution depended on the efficiency of horizontal mixing processes. The vertical density gradient did not have an influence on the flux to the atmosphere in our study.

7.3 Paper 3

Pär Jansson, Bénédicte Ferré, Anna Silyakova, Knut Ola Dølven, Anders Omstedt. ***A new numerical model for understanding free and dissolved gas progression towards the atmosphere in aquatic methane seepage systems***. Submitted to Oceanography and Limnology: Methods

We developed a numerical model which resolves both free and dissolved gas in the water column. It was, to our knowledge, the first model that used multi-size bubbles containing several gas species and which resolved the evolution of dissolved gas while bubbles ascend towards the sea surface. The developed model was used to study the progression of methane gas contained in bubbles escaping from the seafloor. The study included a detailed explanation of the numerical construction and inherent parameterizations, an analysis of the sensitivity to different parameterizations and to environmental conditions. We also compared model output with observations at the slope offshore PKF. In spite of the more complex construction, the numerical precision of M2PG1 compared well with an existing single bubble model (Vielstädte et al., 2015). Like in all Eulerian models, numerical diffusion occurred and the model results can therefore not be directly compared with existing single bubble models. However, the modelled rise height of bubbles compared well with the flare heights seen in the echograms acquired during the CAGE 15-6 cruise. The modelled profiles of dissolved CH_4 compared well (R better than 0.9) with an exponential fit to discrete measurements of CH_4 concentrations collected during the same cruise. The best model fit with observations was achieved with a Gaussian bubble size distribution peaking at 1 mm.

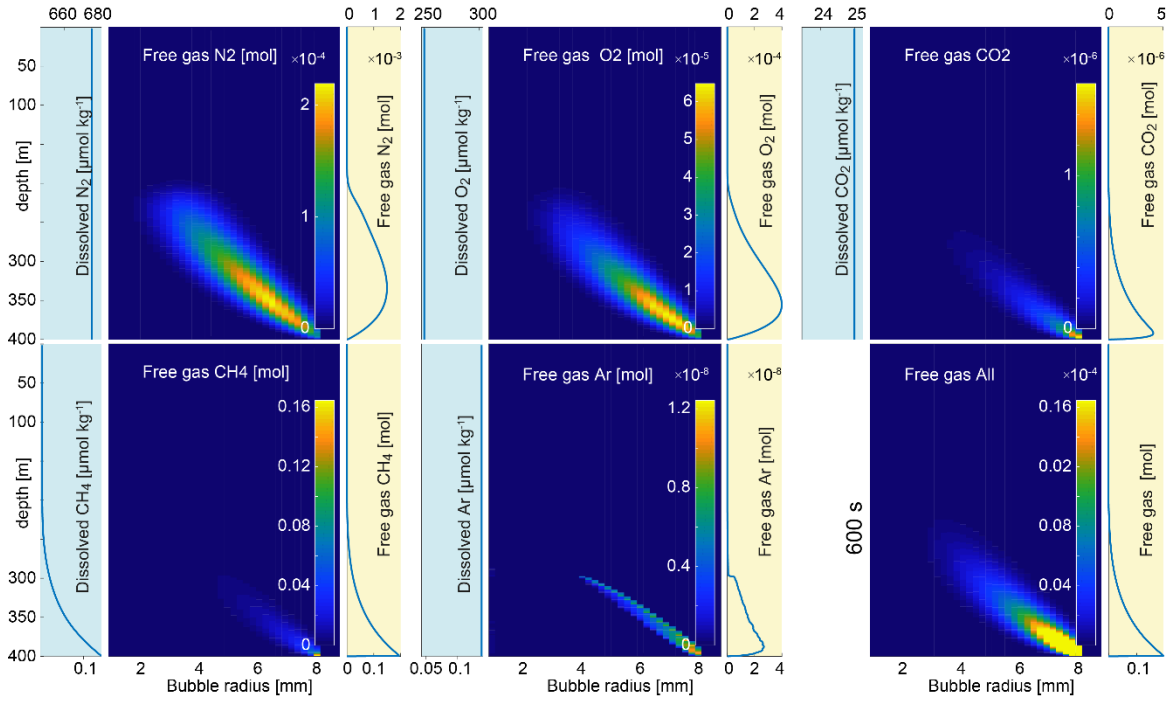

Figure 11. Example of a M2PG1 simulation. Five gas species are represented in their depth- size distribution. Blue to yellow colour scale represents the molar content of free gas in the respective cells. Profiles on yellow background represents the summation of free gas across the bubble sizes at each specific depth. Profiles on blue background shows the dissolved gas concentration. Because the modelled horizontal domain was relatively large, the dissolved gas profiles were largely unaffected by seepage and only the dissolved CH_4 showed an anomaly near the seafloor. The bubble size distribution of the emitted bubbles in this case was single-size of 8 mm equivalent radius.

7.4 Paper 4

Jack Triest, Pär Jansson, Roberto Grilli, Anna Silyakova, Bénédicte Ferré, Jérôme Chappellaz, Jürgen Mienert. **Insights from underwater high resolution dissolved methane sensing over a known methane seepage site west of Svalbard**. In preparation for submission to JGR Ocean

The seepage at the slope offshore PKF was investigated during a three-day campaign in October 2015, using the MILS in addition to our standard oceanographic equipment. The MILS was developed for CH_4 sensing during ice-core drilling in Antarctica. It was designed and built by Jack Triest and Roberto Grilli at the National Centre of Scientific Research in France (https://www.cnrs.fr/), and a modified version was made for seawater deployment, which was tested in July 2014, in the Mediterranean Sea (Grilli et al., submitted). The sensor was, during our survey, for the first time deployed in an environment with substantially CH_4–enriched seawater. The MILS data was in good agreement with sparse discrete sampling and subsequent GC analysis, but MILS revealed unprecedented details of the aqueous CH_4 distribution, both during vertical casts and horizontal towing. Along one of the five horizontal tow-lines (line 3, Figure 12), the CH_4 concentrations were high and the distribution heterogeneous. Simultaneously with towing of the MILS, we monitored echosounder data in real time, which revealed immense CH_4 bubble expulsion along the same line.

Offline flare mapping, using data from the EK60 ship-mounted split-beam echosounder and the Fledermaus software revealed intense flare activity along the slope at about 390 mbsl, which coincided with line 3.

In order to understand the observed heterogeneity, we developed a 2-dimensional model, reconstructing the CH_4 distribution along the tow-line. The 2D model is described in the section *Modelling free and dissolved gas* in the *methods* section of this synthesis. In Paper 4, we report on the 2D modelling procedure and compare the modelled CH_4 distribution with the discrete samples CH_4 and the CH_4 measured with the MILS. The model agreed well with observations but displayed downstream tailing, which we did not see in the MILS data. This is explained by the construction of the model, which only considers turbulent mixing across the domain, whereas, in reality, mixing occurs in all directions.

The analytical solution to the steady state model was calculated by assuming a volume 75 m high, 50 m wide and 4500 m long, which corresponded to the 2D model domain and line 3. In our case the mixing coefficient, *k*, determined by the 2-d modelling, was 1.5 m^2s^{-1}. The observed flow rates were used as input to the volume and the model reached a steady state CH_4 concentration of 23.5 nmol kg^{-1}, twice the background concentration in the area, which was also estimated from the MILS measurements.

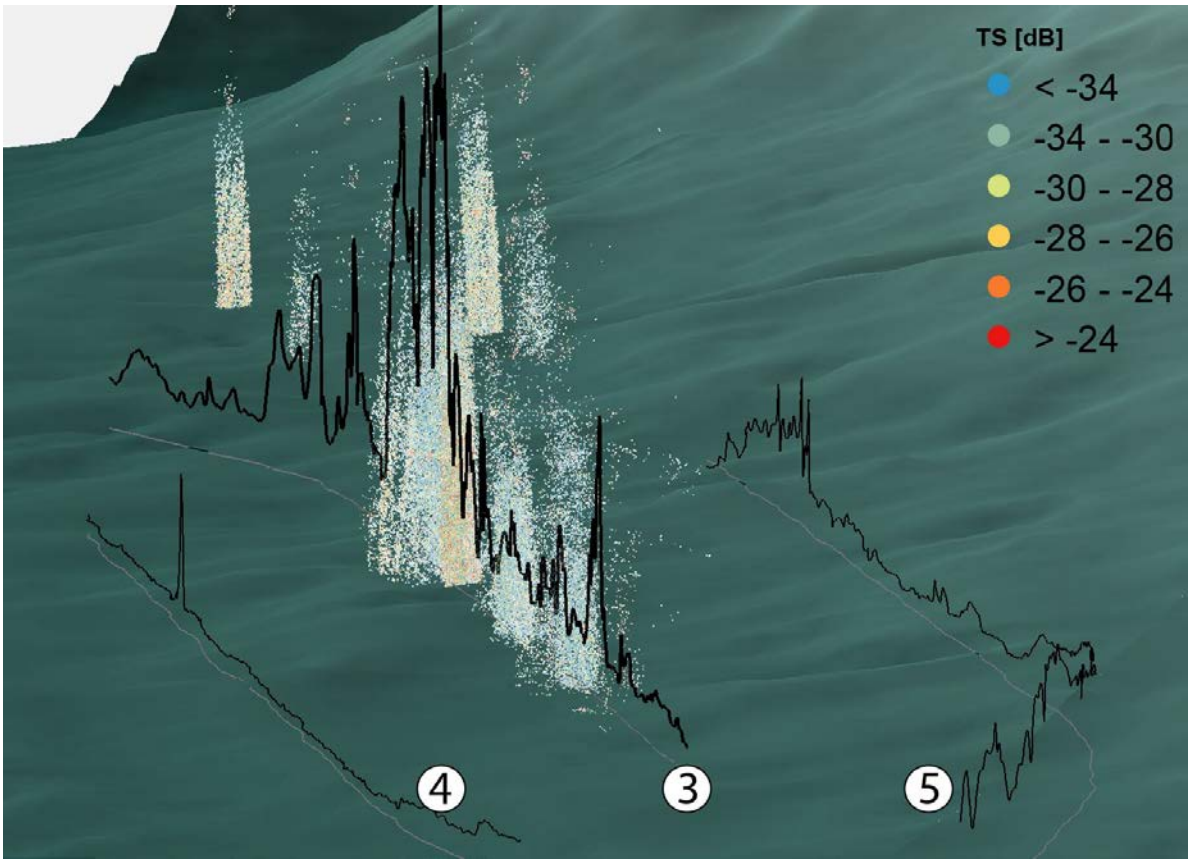

Figure 12. Visualization of gas flares and dissolved CH_4. Target strength (dB) of extracted acoustic data, depicting bubbles in the water column, is shown as coloured dots. Ship track lines 3, 4 and 5, projected on the seafloor, are shown as grey lines and the CH_4 concentration along the lines are shown as black lines.

8 Concluding remarks and outlook

The research conducted during the Ph.D. commitment has substantially improved the understanding of the fate of CH_4 emitted from the seafloor in general and specifically on the western Svalbard continental shelf. We quantified CH_4 emissions from the seafloor and subsequent release to the atmosphere. We compared the variability of CH_4 release with the postulated triggering processes (Paper 1). And developed one- (Paper 3) and two- (Paper 4) dimensional models predicting dissolved CH_4 resulting from free gas emissions from the seafloor. A new fast-response CH_4 sensor was tested (Paper 4) and the data was compared with modelling results with good agreement. Combining the newly developed methods while investigating the same area increased our confidence in the different methods. For example, mapped and quantified CH_4 emissions from the seafloor was incorporated in the new process based 2-phase model and 2D model, which reproduced the observations from high-resolution MILS sensing.

Echosounder data is routinely and extensively collected and used for assessment of fish stocks. Old and new echosounder data could give insights to new CH_4 seepage locations and may help elucidating the development of seepage sites.

Removal rates of CH_4 due to oxidation (MOx) depend on the local CH_4 concentration and the activity of the microbes. MOx can be quantified using ex-situ incubation methods and its efficiency has been noted to increase downstream of CH_4 sources (Mau et al., 2017) as the methanotrophic community grows. Rather than assuming a constant MOx efficiency, the dynamic growth and decay of the methanotrophic community could be included in simulations of future improved versions of M2PG1.

Methane contained in bubbles that are being ejected from the seafloor dissolves in a layer close to the seafloor and a fraction of the dissolved CH_4 is converted to CO_2 due to aerobic oxidation. The additional CO_2 may alter the carbonate system, acidify the seawater, and potentially affect benthic and pelagic ecosystems. Coupling the carbonate system with M2PG1would give increased insight to the acidification effect of CH_4 emissions from the seafloor. CO_2 bubbling from the seafloor can already be modelled with M2PG1 and would possibly be of interest for projects monitoring carbon storage and sequestration.

Future versions of M2PG1 could be used for modelling the fate of substances emitted from the seafloor at hydrothermal vents.

9 References

Andreassen, K., Hubbard, A., Winsborrow, M., Patton, H., Vadakkepuliyambatta, S., Plaza-Faverola, A., Gudlaugsson, E., Serov, P., Deryabin, A., Mattingsdal, R., Mienert, J. & Bünz, S. 2017. Massive blow-out craters formed by hydrate-controlled methane expulsion from the Arctic seafloor. *Science*, 356(6341), pp. 948-953. doi: 10.1126/science.aal4500.

Appen, W.-J. v., Schauer, U., Hattermann, T. & Beszczynska-Möller, A. 2016. Seasonal Cycle of Mesoscale Instability of the West Spitsbergen Current. *Journal of Physical Oceanography*, 46(4), pp. 1231-1254. doi: 10.1175/JPO-D-15-0184.1.

Artemov, Y. G., Egorov, V., Polikarpov, G. & Gulin, S. 2007. Methane emission to the hydro-and atmosphere by gas bubble streams in the Dnieper paleo-delta, the Black Sea.

Berndt, C., Feseker, T., Treude, T., Krastel, S., Liebetrau, V., Niemann, H., Bertics, V. J., Dumke, I., Dünnbier, K., Ferré, B., Graves, C., Gross, F., Hissmann, K., Hühnerbach, V., Krause, S., Lieser, K., Schauer, J. & Steinle, L. 2014. Temporal Constraints on Hydrate-Controlled Methane Seepage off Svalbard. *Science*, 343(6168), p. 284. doi: 10.1126/science.1246298.

Boles, J., Clark, J., Leifer, I. & Washburn, L. 2001. Temporal variation in natural methane seep rate due to tides, Coal Oil Point area, California. *Journal of Geophysical Research: Oceans*, 106(C11), pp. 27077-27086. doi: 10.1029/2000JC000774.

Broecker, W. S. & Peng, T. H. 1974. Gas exchange rates between air and sea1. *Tellus*, 26(1-2), pp. 21-35. doi: 10.3402/tellusa.v26i1-2.9733.

Bünz, S., Polyanov, S., Vadakkepuliyambatta, S., Consolaro, C. & Mienert, J. 2012. Active gas venting through hydrate-bearing sediments on the Vestnesa Ridge, offshore W-Svalbard. *Marine Geology*, 332-334, pp. 189-197. doi: 10.1016/j.margeo.2012.09.012.

Cottier, F., Tverberg, V., Inall, M., Svendsen, H., Nilsen, F. & Griffiths, C. 2005. Water mass modification in an Arctic fjord through cross-shelf exchange: The seasonal hydrography of Kongsfjorden, Svalbard. *Journal of Geophysical Research: Oceans*, 110(C12). doi: 10.1029/2004JC002757.

Egbert, G. D. & Erofeeva, S. Y. 2002. Efficient inverse modeling of barotropic ocean tides. *Journal of Atmospheric and Oceanic Technology*, 19(2), pp. 183-204. doi: 10.1175/1520-0426(2002)019<0183:EIMOBO>2.0.CO;2.

Ferré, B., Mienert, J. & Feseker, T. 2012. Ocean temperature variability for the past 60 years on the Norwegian-Svalbard margin influences gas hydrate stability on human time scales. *Journal of Geophysical Research: Oceans (1978–2012)*, 117(C10). doi: 10.1029/2012JC008300.

Fischer, D., Mogollón, J. M., Strasser, M., Pape, T., Bohrmann, G., Fekete, N., Spiess, V. & Kasten, S. 2013. Subduction zone earthquake as potential trigger of submarine hydrocarbon seepage. *Nature Geoscience*, 6, p. 647. doi: 10.1038/ngeo1886.

Fleming, J. R. 2005. *Historical perspectives on climate change*. Oxford University Press.

Greinert, J., Artemov, Y., Egorov, V., De Batist, M. & McGinnis, D. 2006. 1300-m-high rising bubbles from mud volcanoes at 2080m in the Black Sea: Hydroacoustic characteristics and temporal variability. *Earth and Planetary Science Letters*, 244(1), pp. 1-15. doi: 10.1016/j.epsl.2006.02.011.

Haeckel, M., Suess, E., Wallmann, K. & Rickert, D. 2004. Rising methane gas bubbles form massive hydrate layers at the seafloor. *Geochimica et Cosmochimica Acta*, 68(21), pp. 4335-4345. doi: 10.1016/j.gca.2004.01.018.

Hattermann, T., Isachsen, P. E., Appen, W. J., Albretsen, J. & Sundfjord, A. 2016. Eddy-driven recirculation of Atlantic Water in Fram Strait. *Geophysical Research Letters*, 43(7), pp. 3406-3414. doi: 10.1002/2016GL068323.

Hovland, M. & Thomsen, E. 1997. Cold-water corals—are they hydrocarbon seep related? *Marine Geology*, 137(1-2), pp. 159-164. doi: 10.1016/S0025-3227(96)00086-2.

Hustoft, S., Bünz, S., Mienert, J. & Chand, S. 2009. Gas hydrate reservoir and active methane-venting province in sediments on< 20 Ma young oceanic crust in the Fram Strait, offshore NW-Svalbard. *Earth and Planetary Science Letters*, 284(1), pp. 12-24. doi: 10.1016/j.epsl.2009.03.038.

Kirschke, S., Bousquet, P., Ciais, P., Saunois, M., Canadell, J. G., Dlugokencky, E. J., Bergamaschi, P., Bergmann, D., Blake, D. R., Bruhwiler, L., Cameron-Smith, P., Castaldi, S., Chevallier, F., Feng, L., Fraser, A., Heimann, M., Hodson, E. L., Houweling, S., Josse, B., Fraser, P. J., Krummel, P. B., Lamarque, J.-F., Langenfelds, R. L., Le Quere, C., Naik, V., O'Doherty, S., Palmer, P. I., Pison, I., Plummer, D., Poulter, B., Prinn, R. G., Rigby, M., Ringeval, B., Santini, M., Schmidt, M., Shindell, D. T., Simpson, I. J., Spahni, R., Steele, L. P., Strode, S. A., Sudo, K., Szopa, S., van der Werf, G. R., Voulgarakis, A., van Weele, M., Weiss, R. F., Williams, J. E. & Zeng, G. 2013. Three decades of global methane sources and sinks. *Nature Geoscience*, 6(10), pp. 813-823. doi: 10.1038/ngeo1955.

Kvenvolden, K. A. 1988. Methane hydrate—a major reservoir of carbon in the shallow geosphere? *Chemical Geology*, 71(1), pp. 41-51. doi: 10.1016/0009-2541(88)90104-0.

Kvenvolden, K. A. & Lorenson, T. D. 2001. *The global occurrence of natural gas hydrate*. Wiley Online Library.

Leifer, I. & Patro, R. K. 2002. The bubble mechanism for methane transport from the shallow sea bed to the surface: A review and sensitivity study. *Continental Shelf Research*, 22(16), pp. 2409-2428. doi: 10.1016/S0278-4343(02)00065-1.

Linke, P., Sommer, S., Rovelli, L. & McGinnis, D. F. 2010. Physical limitations of dissolved methane fluxes: The role of bottom-boundary layer processes. *Marine Geology*, 272(1-4), pp. 209-222. doi: 10.1016/j.margeo.2009.03.020.

MacLennan, D. N. 1990. Acoustical measurement of fish abundance. *The Journal of the Acoustical Society of America*, 87(1), pp. 1-15. doi: 10.1121/1.399285.

Magen, C., Lapham, L. L., Pohlman, J. W., Marshall, K., Bosman, S., Casso, M. & Chanton, J. P. 2014. A simple headspace equilibration method for measuring dissolved methane. *Limnol. Oceanogr. Methods*, 12, pp. 637-650. doi: 10.4319/lom.2014.12.637.

Maksimov, A. & Sosedko, E. 2005. Dynamics of sea bubbles covered by a hydrate skin. *XVI Session of the Russian Acoustical Society M*, pp. 459-462.

Mau, S., Römer, M., Torres, M. E., Bussmann, I., Pape, T., Damm, E., Geprägs, P., Wintersteller, P., Hsu, C.-W. & Loher, M. 2017. Widespread methane seepage along the continental margin off Svalbard-from Bjørnøya to Kongsfjorden. *Scientific reports*, 7, p. 42997. doi: 10.1038/srep42997.

McDougall, T. J. & Barker, P. M. 2011. Getting started with TEOS-10 and the Gibbs Seawater (GSW) oceanographic toolbox. *SCOR/IAPSO WG*, 127, pp. 1-28.

McGinnis, D., Greinert, J., Artemov, Y., Beaubien, S. & Wüest, A. 2006. Fate of rising methane bubbles in stratified waters: How much methane reaches the atmosphere? *Journal of Geophysical Research: Oceans (1978–2012)*, 111(C9). doi: 10.1029/2005JC003183.

Medwin, H. & Clay, C. S. 1997. *Fundamentals of acoustical oceanography*. Academic Press.

Nikolovska, A., Sahling, H. & Bohrmann, G. 2008. Hydroacoustic methodology for detection, localization, and quantification of gas bubbles rising from the seafloor at gas seeps from the eastern Black Sea. *Geochemistry, Geophysics, Geosystems*, 9(10). doi: 10.1029/2008GC002118

Pachauri, R. K., Allen, M. R., Barros, V. R., Broome, J., Cramer, W., Christ, R., Church, J. A., Clarke, L., Dahe, Q. & Dasgupta, P. 2014. *Climate change 2014: synthesis report. Contribution of Working Groups I, II and III to the fifth assessment report of the Intergovernmental Panel on Climate Change*. IPCC.

Panieri, G., Bünz, S., Fornari, D. J., Escartin, J., Serov, P., Jansson, P., Torres, M. E., Johnson, J. E., Hong, W. & Sauer, S. 2017. An integrated view of the methane system in the pockmarks at Vestnesa Ridge, 79° N. *Marine Geology*, 390, pp. 282-300. doi: 10.1016/j.margeo.2017.06.006.

Plaza-Faverola, A., Bünz, S., Johnson, J. E., Chand, S., Knies, J., Mienert, J. & Franek, P. 2015. Role of tectonic stress in seepage evolution along the gas hydrate-charged Vestnesa Ridge, Fram Strait. *Geophysical Research Letters*, 42(3), pp. 733-742. doi: 10.1002/2014GL062474.

Portnov, A., Vadakkepuliyambatta, S., Mienert, J. & Hubbard, A. 2016. Ice-sheet-driven methane storage and release in the Arctic. *Nature communications*, 7, p. 10314. doi: 10.1038/ncomms10314.

Rajan, A., Mienert, J. & Bünz, S. 2012. Acoustic evidence for a gas migration and release system in Arctic glaciated continental margins offshore NW-Svalbard. *Marine and Petroleum Geology*, 32(1), pp. 36-49. doi: 10.1016/j.marpetgeo.2011.12.008.

Reeburgh, W. S. 2007. Oceanic Methane Biogeochemistry. *Chemical Reviews*, 107(2), pp. 486-513. doi: 10.1021/cr050362v.

Riedel, M., Wallmann, K., Berndt, C., Pape, T., Freudenthal, T., Bergenthal, M., Bünz, S. & Bohrmann, G. 2018. In Situ Temperature Measurements at the Svalbard Continental Margin: Implications for Gas Hydrate Dynamics. *Geochemistry, Geophysics, Geosystems*, 19(4), pp. 1165-1177. doi: 10.1002/2017GC007288.

Ruppel, C. D. & Kessler, J. D. 2016. The Interaction of Climate Change and Methane Hydrates. *Reviews of Geophysics*. doi: 10.1002/2016RG000534.

Römer, M., Riedel, M., Scherwath, M., Heesemann, M. & Spence, G. D. 2016. Tidally controlled gas bubble emissions: A comprehensive study using long-term monitoring data from the NEPTUNE cabled observatory offshore Vancouver Island. *Geochemistry, Geophysics, Geosystems*, 17(9), pp. 3797-3814. doi: 10.1002/2016GC006528.

Sauter, E. J., Muyakshin, S. I., Charlou, J.-L., Schlüter, M., Boetius, A., Jerosch, K., Damm, E., Foucher, J.-P. & Klages, M. 2006. Methane discharge from a deep-sea submarine mud volcano into the upper water column by gas hydrate-coated methane bubbles. *Earth and Planetary Science Letters*, 243(3-4), pp. 354-365. doi: 10.1016/j.epsl.2006.01.041.

Serov, P., Vadakkepuliyambatta, S., Mienert, J., Patton, H., Portnov, A., Silyakova, A., Panieri, G., Carroll, M. L., Carroll, J., Andreassen, K. & Hubbard, A. 2017. Postglacial response of Arctic Ocean gas hydrates to climatic amelioration. *Proceedings of the National Academy of Sciences*, 114(24), pp. 6215-6220. doi: 10.1073/pnas.1619288114.

Shakhova, N., Semiletov, I., Salyuk, A., Yusupov, V., Kosmach, D. & Gustafsson, Ö. 2010. Extensive Methane Venting to the Atmosphere from Sediments of the East Siberian Arctic Shelf. *Science*, 327(5970), pp. 1246-1250. doi: 10.1126/science.1182221.

Sloan, E. 1998. Physical/chemical properties of gas hydrates and application to world margin stability and climatic change. *Geological Society, London, Special Publications*, 137(1), pp. 31-50.

Steinle, L., Graves, C. A., Treude, T., Ferre, B., Biastoch, A., Bussmann, I., Berndt, C., Krastel, S., James, R. H., Behrens, E., Boning, C. W., Greinert, J., Sapart, C.-J., Scheinert, M., Sommer, S., Lehmann, M. F. & Niemann, H. 2015. Water column methanotrophy controlled by a rapid oceanographic switch. *Nature Geosci*, 8(5), pp. 378-382. doi: 10.1038/ngeo2420.

van Oevelen, D., Bergmann, M., Soetaert, K., Bauerfeind, E., Hasemann, C., Klages, M., Schewe, I., Soltwedel, T. & Budaeva, N. E. 2011. Carbon flows in the benthic food web at the deep-sea

observatory HAUSGARTEN (Fram Strait). *Deep Sea Research Part I: Oceanographic Research Papers*, 58(11), pp. 1069-1083. doi: 10.1016/j.dsr.2011.08.002.

Veloso, M., Greinert, J., Mienert, J. & De Batist, M. 2015. A new methodology for quantifying bubble flow rates in deep water using splitbeam echosounders: Examples from the Arctic offshore NW-Svalbard. *Limnology and Oceanography: Methods*. doi: 10.1002/lom3.10024.

Vielstädte, L., Karstens, J., Haeckel, M., Schmidt, M., Linke, P., Reimann, S., Liebetrau, V., McGinnis, D. F. & Wallmann, K. 2015. Quantification of methane emissions at abandoned gas wells in the Central North Sea. *Marine and Petroleum Geology*. doi: 10.1016/j.marpetgeo.2015.07.030.

Wallmann, K., Riedel, M., Hong, W., Patton, H., Hubbard, A., Pape, T., Hsu, C., Schmidt, C., Johnson, J. & Torres, M. 2018. Gas hydrate dissociation off Svalbard induced by isostatic rebound rather than global warming. *Nature communications*, 9(1), p. 83. doi: 10.1038/s41467-017-02550-9.

Wanninkhof, R. 2014. Relationship between wind speed and gas exchange over the ocean revisited. *Limnology and Oceanography: Methods*, 12(6), pp. 351-362. doi: 10.4319/lom.2014.12.351.

Weber, T. C., Mayer, L., Jerram, K., Beaudoin, J., Rzhanov, Y. & Lovalvo, D. 2014. Acoustic estimates of methane gas flux from the seabed in a 6000 km2 region in the Northern Gulf of Mexico. *Geochemistry, Geophysics, Geosystems*. doi: 10.1002/2014GC005271.

Westbrook, G., Chand, S., Rossi, G., Long, C., Bünz, S., Camerlenghi, A., Carcione, J., Dean, S., Foucher, J.-P. & Flueh, E. 2008. Estimation of gas hydrate concentration from multi-component seismic data at sites on the continental margins of NW Svalbard and the Storegga region of Norway. *Marine and Petroleum Geology*, 25(8), pp. 744-758. doi: 10.1016/j.marpetgeo.2008.02.003.

Westbrook, G. K., Thatcher, K. E., Rohling, E. J., Piotrowski, A. M., Pälike, H., Osborne, A. H., Nisbet, E. G., Minshull, T. A., Lanoisellé, M. & James, R. H. 2009. Escape of methane gas from the seabed along the West Spitsbergen continental margin. *Geophysical Research Letters*, 36(15). doi: 10.1029/2009GL039191.

Paper 1

Paper 2

Paper 3

Paper 4